

## Glycolipid Biotinylation on Purple Membrane with Maintained Bioactivity

Yan Xiang,<sup>\*,†,‡</sup> Meng Yang,<sup>‡</sup> Tao Su,<sup>§</sup> Yuanyuan Chen,<sup>§</sup> Lijun Bi,<sup>§</sup> and Kunsheng Hu<sup>\*,§</sup>

School of Chemistry and Environment, Beihang University, Beijing, P. R. China 100191, School of Materials Science and Engineering, Beihang University, Beijing, P. R. China 100191, and Institute of Biophysics, Chinese Academy of Sciences, Beijing, P. R. China 100101

Received: February 16, 2009; Revised Manuscript Received: April 23, 2009

In this study, labeled purple membrane (PM, *Halobacterium salinarum*) patches with maintained bioactivity were prepared by biotinylation of the glycolipids on the extracellular (EC) surface of the PM. After in situ streptavidin incubation, the extracellular surface could be directly visualized because it was completely covered with bright dots. The height of a single biotin/streptavidin interaction layer was approximately 2.5 nm. By using calcium thioglycolate-modified tips and an atomic-force microscope (AFM), two distinct topographical features of PMs placed in a buffer with low salt concentration were recognized: the flat EC surface and the domelike cytoplasmic (CP) surface. Biotinylation and AFM with modified tips were simultaneously used with consistent results. Those observations are useful for future studies on PM bioconjugation and oriented assembly as well as the design of bacteriorhodopsin-based photoelectric devices.

## 1. Introduction

Bacteriorhodopsin (BR) is the only integral membrane protein in the purple membrane (PM), which has been isolated from the cell membranes of *Halobacterium salinarum*.<sup>1</sup> BR is a very promising biomaterial and has attracted considerable interest in the fields of biooptics<sup>2–5</sup> and bioelectronics.<sup>6–10</sup> This is because BR shows long-term stability against thermal, chemical, and photochemical degradation and exhibits desirable photoelectric and photochromic properties in addition to the ability to maintain its biological activity when immobilized on solid substrates.

In order to efficiently generate electric responses using BR-based photoelectric devices and other BR-based instruments, it is essential that a nonrandomly oriented BR film be prepared. To construct a highly oriented film of PM, Langmuir–Blodgett (LB) deposition,<sup>10,11</sup> electrophoretic sedimentation (EPS),<sup>5,12,13</sup> electrostatic layer-by-layer (LBL) adsorption,<sup>8,14</sup> preferential orientation at interfaces,<sup>15</sup> immobilizing matrixes,<sup>16</sup> sol–gel encapsulation,<sup>17</sup> and molecular recognition<sup>4,18,19</sup> techniques have been applied.

We have prepared highly oriented films of PM patches by using a biotin/streptavidin molecular recognition technique and found that biotinylation did not obviously affect the photochemical activity of BR.<sup>4</sup> The oriented PM film exhibited a remarkably higher photoelectric voltage than a nonspecific-labeled film. A further study<sup>20</sup> using BR labeled by streptavidin-bound biotin revealed that biotin molecules covered both surfaces of the PM, but the amount of biotinylated BR on the extracellular (EC) surface was markedly higher than that on the cytoplasmic (CP) surface. Importantly, when fluorescamine was used, only the CP surface was selectively biotinylated; the proton conductivity and activity of the PM was reduced by 50%.

The wild-type PM has a two-dimensional hexagonal crystalline lattice structure consisting of three single BR molecules and 30 lipid molecules.<sup>21</sup> A complex glycosulphospholipid and S-TGA-1 (3HSO<sub>3</sub>-Galp- $\beta$ 1, 6-Manp- $\alpha$ 1, 2-Glcp- $\alpha$ 1, 1-*sn*-2, 3-diphytanylglycerol) are present in the PM, and S-TGA-1 is located on its EC surface.<sup>22,23</sup> Further studies have suggested that S-TGA-1 is located on both the internal and external surfaces of BR crystalline lattices.<sup>21,24</sup> Henderson et al.<sup>22</sup> have proved that, after modification with biotin *N*-hydroxysuccinimide ester, BR could be asymmetrically biotinylated on the EC surface of the PM rather than on the CP surface under alkaline conditions (pH 8.5–9.0). The addition of sodium periodate inhibited the biotinylation of BR and resulted in the selective labeling of the glycolipids in the PM.

In recent years, atomic-force microscopy (AFM) has become an important and powerful tool to study biological samples. It is possible to differentiate the structural differences between EC and CP with high-resolution imaging which is not always accessible.<sup>25–28</sup> In order to develop more effective labeling methods that do not produce functional impairment of BR, we selectively labeled the EC surfaces of PM patches through the biotinylation of the glycolipid. By using AFM, we directly observed the remarkable changes in the surface topography of the PM after the biotinylation of the glycolipids in the PM. We found that biotin molecules were only attached to the EC surface of the PM and the bioactivity of the PM was maintained. Differences on the topography of the biotinylated PM were also studied using AFM with modified tips.

## 2. Materials and Methods

**2.1. Materials and Reagents.** The PM was isolated from the R<sub>1</sub>M<sub>1</sub> strain of *H. salinarum*, using standard procedures,<sup>29</sup> and stored in double-distilled water at 4 °C. Streptavidin was purchased from Sigma-Aldrich. Biotin hydrazide was purchased from Molecular Probes. Other reagents were purchased from Fluka. Streptavidin solution (50  $\mu$ g/mL) was prepared using 10 mM phosphate buffer (pH 7.6). Mica sheets were treated using the standard method.<sup>4,20</sup>

\* To whom correspondence should be addressed. Tel/Fax: 861082339539 (Y.X. and K.H.). E-mail: xiangy@buaa.edu.cn (Y.X.); huks@sun5.ibp.ac.cn (K.H.).

<sup>†</sup> School of Chemistry and Environment, Beihang University.

<sup>‡</sup> School of Materials Science and Engineering, Beihang University.

<sup>§</sup> Chinese Academy of Sciences.

## 2.2. Reaction of Wild-Type PM with Biotin Hydrazide.

The biotin-labeling procedure of Richard Henderson was followed.<sup>22</sup> In brief, 1 mL of a 4 mg/mL suspension of PM was added to a 2 mL reaction tube containing a stir bar and was mixed with 12 mM sodium periodate in phosphate-buffered saline (PBS) buffer (pH 7.3). After stirring for 1 h, the solution was centrifuged and resuspended in PBS buffer twice. Subsequently, 100  $\mu$ L of freshly prepared biotin hydrazide solution (50  $\mu$ g/mL) was added to the reaction tube, and the solution was stirred for 2 h at room temperature; the sample was then centrifuged at 20 000 rpm for 10 min and resuspended in PBS. The sample was washed three times using centrifugation and resuspended in PBS buffer (pH 7.3) to remove excess biotin, which had weakly coupled to the hydroxyl groups in the membrane. Finally, the sample was dialyzed against 10 mM PBS buffer for 2 days at 4 °C.

**2.3.  $M_{412}$  and Proton-Pump Activity.** We used time-resolved kinetic spectra to measure the transient accumulation of  $M_{412}$  and the proton-pump activity of BR with homemade instruments.<sup>4,20</sup> The wavelength of the stimulating light was 570 nm and that of the probing light was 412 nm. All measurements were carried out at room temperature. Pyranine was used as an excellent pH probe in proton pump function detection. The results were analyzed by the method of Govindjee et al.<sup>30</sup> The characteristic absorption wavelengths of both the PM and biotin-labeled PM were measured using the Hitachi U-3200 spectrophotometer. All measurements were taken at room temperature.

**2.4. Surface Plasmon Resonance Analysis.** Surface plasmon resonance (SPR) experiments were carried out at 25 °C using BIAcore 3000 (BIAcore AB, Uppsala, Sweden). The running buffer, PBS, was prepared, vacuum filtered, and degassed immediately prior to use. Streptavidin-modified chips (SA chips) preconditioned by three consecutive 1 min pulses of 1 M NaCl in 50 mM NaOH were used to exclude nonspecific adsorption between the wild-type PM and streptavidin. The PBS buffer, the PM in deionized (DI) water, and the biotinylated PM in the running buffer were injected over the sensor chip surface for 4 min at 30  $\mu$ L/min, followed by 6 min of buffer flow. All data were analyzed by using the BIA evaluation 4.1 software to obtain corrected sensorgrams.

**2.5. AFM.** The surface morphology of the PM was examined with a commercial atomic-force microscope (NanoScope IIIa and Multi-Mode AFM; Digital Instruments) equipped with a 13  $\mu$ m scanner and liquid sample holder. Oxidized sharpened  $\text{Si}_3\text{N}_4$  tips (NP-S) with an elastic constant of 0.06 N/m were used in this experiment. In tapping mode, the driven frequency was set to 8.5 kHz to avoid unwanted resonance peaks caused by cantilever adjustments. The set-point value was adjusted as needed. The deflection sensitivity of the cantilever was adjusted according to the stress curve obtained on the mica sheet.

The biotinylated PM suspension was diluted to 0.1 mg/mL with a buffer of 25 mM KCl and 10 mM Tris, pH 7.6 for imaging. Subsequently, 10  $\mu$ L of diluted suspension was deposited on a freshly prepared mica sheet, which was glued to a steel disk and magnetically mounted onto the piezoelectric ceramic scanner. Next, 30  $\mu$ L of buffer was injected into the holder. The sample was left for 30 min to attain thermal balance. Images were processed using the software provided with the NanoScope instrument. First-order flattening and the erase scan line command were used as needed.

A novel tip-modified method was developed in our group to strengthen the electrostatic repulsion between tips and the PM.<sup>31</sup> The tips were gold plated, dipped into 0.1 M HCl for a few seconds, and washed with 10 mM sodium phosphate buffer (pH

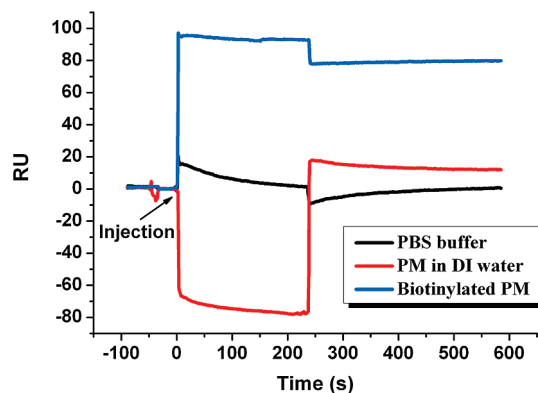


**Figure 1.** SPR spectra of the natural PM and biotinylated glycolipid PM on streptavidin substrate chips.

7.2). Subsequently, the tips were immersed into 3.2 mM calcium thioglycolate solution for 1 h at room temperature and washed with 10 mM sodium phosphate buffer (pH 7.2) and then with distilled water to remove the unreacted calcium thioglycolate. For the modified tips, PM samples were prepared in buffers with needed KCl concentration.

## 3. Results and Discussion

**3.1. Exclusion of Nonspecific Adsorption.** With the help of AFM, the affinity of antigen–antibody interactions and the sensitivity of optical characters can be used to differentiate the surface of the PM. It has been found that BR lost 50% of its activity after direct biotinylation on the BR protein.<sup>20</sup> In this study, the glycolipids on the EC surface of the PM were selectively biotinylated. To confirm this selective biotinylation, the effect of the specific interaction between the streptavidin substrate and the PM was excluded. We used SPR to monitor the in situ intermolecular interaction between the PM and the streptavidin substrate under the same conditions. The results are shown in Figure 1. Binding was quantified as an increase in the response units (RUs) at 60 s after the end of the injection over the RUs at the baseline, i.e., at 20 s prior to the injection (Figure 1). The bulk at the injection start and end points was mostly due to the differences in the refractive indices of the sample (water or sample concentrations) and PBS buffer. The above findings show that nonspecific adsorption only slightly existed between the wild-type PM and streptavidin. This finding is consistent with our previous result that very little nonspecific adsorption occurred, and that the adsorption may be attributed to both electrostatic attraction and hydrophobic interaction.<sup>4</sup> Specific binding is mainly between the biotinylated PM and streptavidin with high affinity.<sup>32,33</sup>

**3.2. Characterization by AFM.** **3.2.1. Glycolipid Biotinylation.** The surface morphology of the biotinylated PM was analyzed using high-resolution AFM. The surfaces of labeled PM patches were smooth and flat with a diameter of 1  $\mu$ m and vertical roughness of 0.5 nm (Figure 2A). After the in situ incubation of streptavidin for 30 min, some specific regions of the PM patches in the scanning area became rougher and were covered by bright dots with a diameter of 15 nm and a height of 3 nm, shown as Figure 2B, while the other patches remained smooth. Previous studies have proved that glycolipids are located only on the EC surface of the PM, and that biotin hydrazide can specifically react with the glycolipids in sodium periodate-treated PMs.<sup>22</sup> Thus, streptavidin molecules are only distributed on the biotinylated EC surface of PM patches. Here, the height of a single biotin/streptavidin interaction layer was estimated to be 2.5 nm.<sup>34</sup> This partially explains the substantial differences

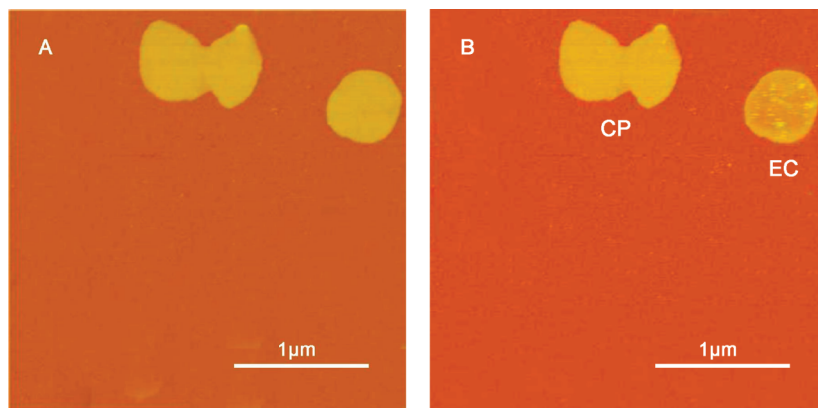


**Figure 2.** Surface morphology of biotinylated glycolipids on PM patches before (A) and after (B) streptavidin incubation, as evaluated using AFM in 25 mM KCl Tris buffer at pH 7.65, 25 °C. The EC surface of labeled PM patch covered by shine dots.

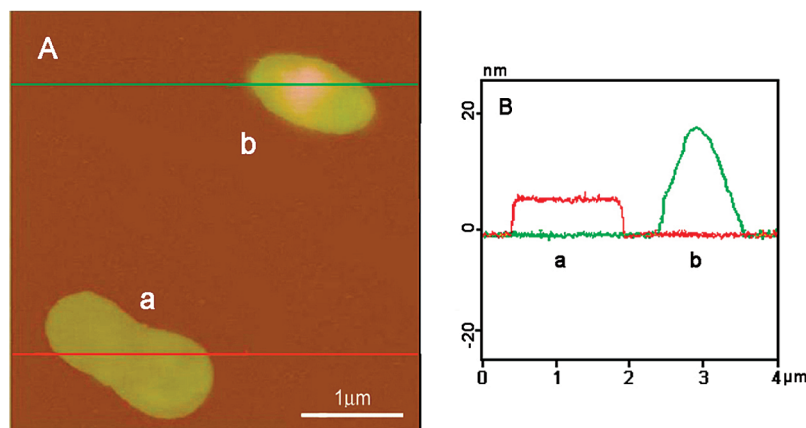


**Figure 3.** Surface morphology (A) of biotinylated glycolipid PM patches in 25 mM KCl buffer with modified AFM tip, in the tapping mode with a set-point value of 1.8 V. Elevation profile of PM patches (B). Patch a is flat with an average height of 6 nm. Patch b is bell shaped with a central height of 20 nm.

among the AFM images. The PM patches with the highlighted spots were the EC surface, and the smooth patches were the CP surface. In situ incubation of streptavidin with biotinylated glycolipids can be an efficient method to differentiate between the EC and CP surfaces of PM patches.

**3.2.2. Changes in PM Morphology As Examined Using AFM with a Modified Tip.** The type of tips used and the experimental conditions are very important and affect the final image; they can also provide useful information about membrane structure, molecular interactions, etc. In recent years, AFM has evolved from an imaging method to a multifunctional “laboratory on a tip” that allows the observation and manipulation of the machinery of cellular membranes.<sup>28</sup> To develop a novel analysis method, the influence of salt concentration and set-point values on the morphology of the biotinylated PM were considered. The PM is negatively charged and the magnitude of the charge on the EC surface is lower than that on the CP surface.<sup>35,36</sup> In a buffer with a low salt concentration (25 mM KCl and 10 mM Tris, pH 7.6), the electron charges on the PM were not completely masked by the ions in the buffer. Hence, the calcium thioglycolate-modified tips, which carried a negative charge, could affect the electronegative CP surface, leading to changes in the PM morphology. In contrast, such electrostatic repulsion did not occur between the EC surfaces and the negatively charged tips because the weak negative charge on the EC surface was completely masked in the buffer. The difference between morphology of the two surfaces could be visualized using the elevation map of AFM.

Figures 3 and 4 show the surface morphology of labeled PM patches in 25 mM KCl buffer obtained at different set-point values. When the set-point value was 1.8 V, patch a was flat, while patch b was domelike. In Figure 3B, the profiles of the PM patches are shown; the difference in the heights of the patches can be clearly seen. The red line represents patch a, which has an average height of 6 nm;<sup>6,37,38</sup> the deviation in the height did not exceed 0.5 nm. The green line represents patch b, which has a central height of 20 nm. When the set-point value was reduced, i.e., the tap force was increased, the height of patch b decreased. When the set-point value was reduced to 1.5 V (Figure 4), the height of patch b decreased to 6 nm, which equals the height of the native patch. Patch b regained its original shape when the set-point value was reset to 1.8 V; in contrast, the shape of patch a did not change during the entire process. These phenomena indicated that the changes in the morphology of patch b resulted from electrostatic repulsion between the modified tip and the CP surface. Therefore, we concluded that the upper surface of patch b was the CP surface and that of patch a was the EC surface. The negative charge on the latter was smaller than that on the former. The same phenomena was also found in natural PM,<sup>31</sup> which illustrated that the biotinylation of glycolipid on the specific EC side did not affect the structural and charge character of the CP surface. This technique provides an easy, reliable, and efficient method to identify the surfaces of PM patches in buffers with low salt concentrations.

Normally, high-resolution imaging of the PM can only be obtained in buffers of high salt concentration which screen off the electrostatic interaction between the AFM tip and PM



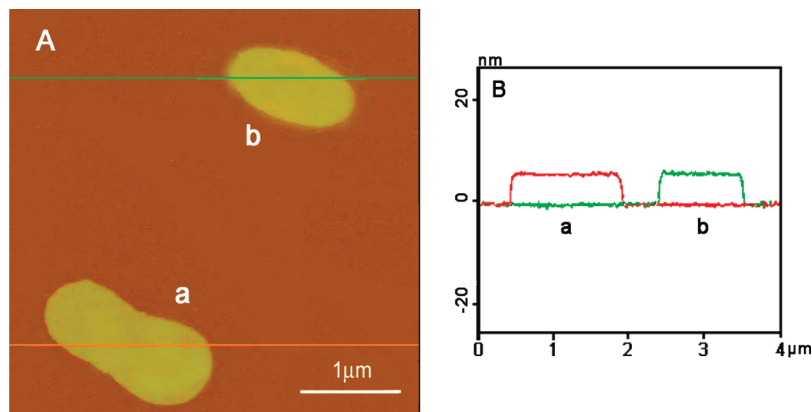


**Figure 4.** Surface morphology (A) of biotinylated glycolipid PM patches in 25 mM KCl buffer with modified AFM tip, in the tapping mode with a set-point value of 1.5 V. Elevation profile of PM patches (B). Patches a and b are equally thick (6 nm).

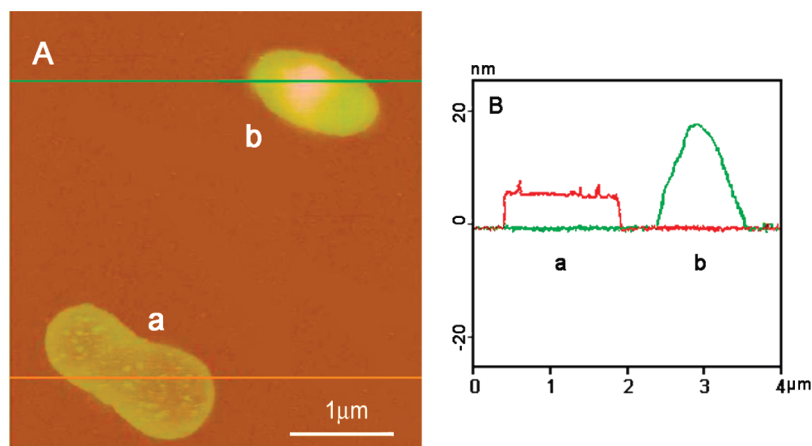


**Figure 5.** Surface morphology (A) of biotinylated glycolipid PM patches in 25 mM KCl buffer after incubation of streptavidin 30 min with modified AFM tip, in the tapping mode with a set-point value of 1.8 V. Elevation profile of PM patches (B). Patch a is flat, rough with covered bright dots. Patch b is smooth and domelike with a central height of 20 nm.

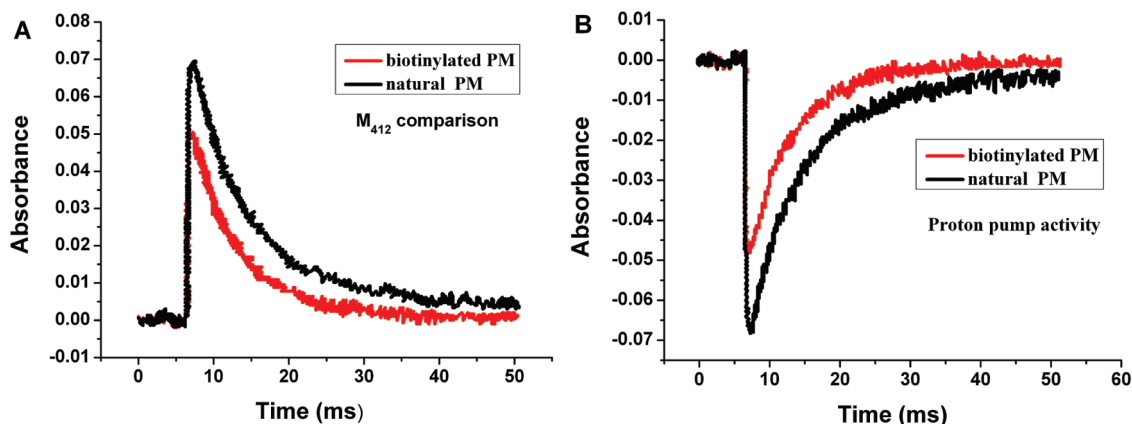


**Figure 6.** (A)  $M_{412}$  yield from biotin-labeled glycolipids in PM patches was approximately 70% of that from the wild-type PM at the same BR concentration. (B) The proton-pump activity of the PM with biotin-labeled glycolipids was approximately 70% of that of the wild-type PM at the same BR concentrations.

surface.<sup>38,39</sup> With the modified tip and the buffer having a higher salt concentration (>50 mM KCl), the repulsion between the tip and PM disappeared since the ions completely masked the negative charges on the PM. No domelike surface formed at any set-point value. All PM patches were of the same height, 6 nm, which equals the height of the wild-type PM.

**3.2.3. Evaluation of Glycolipid Biotinylation by AFM with Modified Tips.** Streptavidin was added to the sample holder containing the biotinylated glycolipid PM, and the PM patches were imaged using AFM with calcium thioglycolate-modified

tips. At a set-point value of 1.8 V (Figure 5), patch a was flat and rough with an average height of 6 nm and covered with shining dots that represented biotin-streptavidin interactions. These findings indicate that the upper surface of patch a is the EC surface. In contrast, patch b was smooth and domelike, which indicated that its upper surface was the CP surface. Thus, the results of two modification methods were consistent, and hence, the validity of both methods was confirmed.

We developed efficient methods to identify the surface of PM patches; these methods can suit different requirements. The

glycolipid biotinylation method can be used without limits of buffer concentration or tips. The modified tips method can be used directly to image samples without incubation of the samples containing streptavidin in a low salt concentration buffer.

**3.3. Examination of the Functions of Labeled PMs.** It is important to examine the bioactivity and function of the modified PM which helps to evaluate the injury induced by modification methods. The photochemical cycle of BR can be characterized by flash photolysis kinetic spectra that represent the decay of  $M_{412}$ , an intermediate in the photocycle. The relative concentrations of  $M_{412}$  and its half life can be determined by time-resolved kinetics, which could facilitate the assessment of PM bioactivity. In our experiments, as shown in Figure 6A, the yield (absorbance) of  $M_{412}$  from the biotinylated PM was approximately 70% of that from the wild-type PM. The curves of  $M_{412}$  obtained from the wild-type and biotinylated glycolipid PMs fitted exponential decay functions with half-lives of 4.1 and 4.3 ms, respectively. These findings suggest that  $M_{412}$  and its related intermediates are not greatly disturbed by biotinylation of glycolipid processes. Identical results were obtained with regard to the proton-pump activity of the PM (Figure 6B). The time-resolved kinetic spectra of glycolipids in the biotinylated PM showed that the absorbance of the PM was approximately 70% that of the wild-type PM. Thus, the proton-pumping ability of the biotin-labeled PMs was maintained, but the activity of the proton pump was reduced in some degree. This functional preservation may be explained by the fact that the glycolipids around BR were biotinylated, and the BR proton channels were not blocked to as great of an extent as in previously used methods.<sup>20</sup> Compared with the direct biotinylation of BR protein, biotinylation of glycolipids resulted in a lower degree of functional impairment, which is an advantage of this labeling method.

The visible ultraviolet (UV-vis) specific absorption peaks of the PM remained unchanged after biotinylation glycolipids of the membrane, and the absorbance of BR at A280/A568 was almost unchanged as well. These findings indicate that the biotinylation of the glycolipid had almost no obviously negative influence on the photochemical properties of BR and the covalent binding of glycolipids.

#### 4. Conclusions

By using AFM techniques, glycolipid biotinylation on the extracellular surface of the purple membrane could be visualized since it was uniformly covered with bright dots after in situ streptavidin incubation. The height of a single biotin/streptavidin interaction layer was approximately 2.5 nm. With a modified tip, the cytoplasmic surface of the labeled purple membrane was directly identified in the low salt concentration due to its specific domelike appearance; its structural and charge characters were not affected by biotinylation. Glycolipid biotinylation of the EC surface and the modified tips methods can be used synergistically to identify PM surfaces with good reliability and feasibility.

Few studies have attempted to determine whether biotinylation of glycolipid affected the structure and functions of BR. In this study, the analysis of UV-vis and kinetic spectra of  $M_{412}$  suggested that the essential photocycle properties of BR were only slightly affected by biotinylation. An approximately 30% decrease in the  $M_{412}$  yield and proton-pump activity was observed after glycolipid biotinylation. Very little nonspecific adsorption occurred between the wild-type PM and streptavidin. The results could provide useful information for the ordered assembly of PMs in biochips, photoelectric devices, or other applications.

**Acknowledgment.** We thank Dr. Sheng Zhong in Prof. K.H.'s lab for the AFM tip modification. This work was

supported by grants from the National Natural Science Foundation of China (No. 20403002 and No. 20773008), the National High-tech R&D Program (863 Program) (No. 2007AA05Z146), Beijing Novel Program (2008B12), and The 973 Project of the Ministry of Science and Technology of China (No.2007CB935703).

#### References and Notes

- (1) Stoeckenius, W.; Lozier, H. R.; Bogomolri, A. P. *Biochim. Biophys. Acta* **1979**, *505*, 215.
- (2) Brige, R. R. *Nature* **1994**, *371*, 659.
- (3) Fukuzawa, K.; Yanagisawa, K.; Kuwano, H. *Sens. Actuators, B* **1996**, *30*, 121.
- (4) Chen, D. L.; Lu, Y. J.; Sui, S. F.; Xu, B.; Hu, K. S. *J. Phys. Chem. B* **2003**, *107*, 3598.
- (5) Li, R.; Li, C. M.; Bao, H. F.; Bao, q. L.; Lee, S. V. *Appl. Phys. Lett.* **2007**, *91*, 223901.
- (6) He, T.; Friedman, N.; Cahen, D.; Sheves, M. *Adv. Mater.* **2005**, *17* (8), 1023.
- (7) Ermolina, I.; Lewis, A.; Feldman, Y. *J. Phys. Chem. B* **2003**, *107*, 14537.
- (8) He, J. A.; Samuelson, L.; Li, L.; Kumar, J.; Tripathy, K. S. *Langmuir* **1998**, *14*, 1674.
- (9) Jin, Y. D.; Friedman, N.; Sheves, M.; Cahen, D. *Adv. Funct. Mater.* **2007**, *17* (8), 1417.
- (10) Miyasaka, T.; Koyama, K. *Thin Solid Films* **1992**, *210*, 146.
- (11) Miyasaka, T.; Koyama, K.; Itoh, I. *Science* **1992**, *255*, 342.
- (12) Keszthelyi, L. *Biochim. Biophys. Acta* **1980**, *598*, 429.
- (13) Wang, J. P.; Yoo, S. K.; Song, L.; ElSayed, M. A. *J. Phys. Chem. B* **1997**, *101*, 3420.
- (14) He, J. A.; Samuelson, L.; Li, L.; Kumar, J.; Tripathy, S. K. *Adv. Mater.* **1999**, *11*, 435.
- (15) Fisher, K. A.; Yanagimoto, K.; Stoeckenius, W. *J. Cell. Biol.* **1978**, *77*, 611.
- (16) Chen, Z.; Lewis, A.; Takei, H.; Nebenzahl, I. *Appl. Opt.* **1991**, *30*, 5188.
- (17) Wu, S. G.; Ellerby, L. M.; Cohan, J. S.; Dunn, B.; El-Sayed, M. A.; Valentine, J. S.; Zink, J. I. *Chem. Mater.* **1993**, *5*, 115.
- (18) Koyama, K.; Yamaguchi, N.; Miyasaka, T. *Adv. Mater.* **1995**, *7*, 590.
- (19) Koyama, K.; Yamaguchi, N.; Miyasaka, T. *Science* **1994**, *265*, 762.
- (20) Su, T.; Zhong, S.; Zhang, Y.; Hu, K. S. *J. Photochem. Photobiol., B* **2008**, *92* (2), 123.
- (21) Corcelli, A. V.; Lattanzio, T. M.; Mascolo, G.; Papadia, P.; Fanizzi, F. *J. Lipid Res.* **2002**, *43*, 132.
- (22) Henderson, R.; Jubb, J. S.; Whytock, S. *J. Mol. Biol.* **1978**, *123*, 259.
- (23) Corcelli, A. V.; Colella, M.; Mascolo, G.; Fanizzi, F. P.; Kates, M. *Biochemistry* **2000**, *39*, 3318.
- (24) Weik, M.; Patzelt, H.; Zaccari, G.; Oesterhelt, D. *Mol. Cell* **1998**, *1* (3), 411.
- (25) Voitchovsky, K.; Contera, S. A.; Kamihira, M.; Watts, A.; Ryan, J. F. *Biophys. J.* **2006**, *90* (6), 2075.
- (26) Müller, D. J.; Heymann, J. B.; Oesterhelt, F.; Möller, C.; Gaub, H.; Büldt, G.; Engel, A. *Biochim. Biophys. Acta* **2000**, *1460* (1), 27.
- (27) Müller, D. J.; Sass, H.-J.; Müller, S.; Büldt, G.; Engel, A. *J. Mol. Biol.* **1999**, *285*, 1903.
- (28) Müller, D. J. *Biochemistry* **2008**, *47* (31), 7986.
- (29) Oesterhelt, D.; Stoeckenius, W. *Methods Enzymol.* **1974**, *31*, 667.
- (30) Govindjee, R.; Ebrey, T. G.; Crofts, A. R. *Biophys. J.* **1980**, *30*, 231.
- (31) Zhong, S.; Li, H.; Cheng, X. Y.; Cao, E. H.; Jin, G.; Hu, K. S. *Langmuir* **2007**, *23*, 4486.
- (32) Green, M. N. *Adv. Protein Chem.* **1975**, *29*, 85.
- (33) Weber, C. P.; Ohlendorf, D. H.; Wendoloski, J. J.; Salemme, R. F. *Science* **1989**, *243*, 85.
- (34) Lee, U. G.; Kidwell, A. D.; Colton, J. R. *Langmuir* **1994**, *10* (2), 354.
- (35) Alexiev, T.; Marti, T.; Heyn, M. P.; Khorana, H. G.; Scherrert, P. *Biochemistry* **1994**, *33* (46), 298.
- (36) Jonas, R.; Kautalos, Y.; Ebrey, T. G. *Photochem. Photobiol.* **1990**, *52*, 1162.
- (37) Hampp, N. *Nature* **1993**, *366*, 12.
- (38) Muller, D. J.; Engel, A. *Biophys. J.* **1997**, *73* (3), 1633.
- (39) Kienberger, F.; Stroh, C.; Kada, G.; Moser, R.; Baumgartner, W.; Pastushenko, V.; Rankl, C.; Schmidt, U.; Muller, H.; Orlova, E.; Legrimel-lec, C.; Drenckhahn, D.; Blaas, D.; Hinterdorfer, P. *Ultramicroscopy* **2003**, *97*, 229.